

Space-Charge-Limited Current in Neutron-Irradiated Silicon, with Evidence of the Complete Lampert Triangle*

H. THURMAN HENDERSON† AND K. L. ASHLEY

Southern Methodist University, Electronic Sciences Center, Dallas, Texas 75222

(Received 17 March 1969)

A theoretical model proposed by Lampert in 1956 suggests that all single-carrier conduction possibilities in solids, with discrete trapping levels and under constant mobility, are limited within a triangular region on a log-current-versus-log-voltage plot. Lampert's triangle is bounded by Ohm's law, Child's trap-free square law for solids, and an essentially vertical traps-filled-limit line. This paper reports the experimental observation of two of the bounding sides of this triangle, with the theoretically calculated third side fitting the experimental data very well, when based upon measured parameters using two methods of attack. The observations were made on a fast-neutron-irradiated silicon chip with gold-alloy electrodes, at 77°K. The behavior is principally due to the trapping character of the well-known oxygen-vacancy *A* center, which is activated by the neutron irradiation.

INTRODUCTION

OVER ten years ago, Lampert theorized that single-carrier injection into solids (insulators, in particular) is confined to a triangular region in a log-current-versus-log-voltage plot.¹ This triangle, as shown in Fig. 1, is bounded by Ohm's law, Child's trap-free square law for solids, and a traps-filled-limit (TFL) curve, which is an essentially vertical rise in current at voltage V^{TFL} . The specific location of possible curves within the triangular region depends upon the density and location of the particular trapping level within the energy gap, as well as the thermal-equilibrium free-carrier density. However, within the triangle, the specific curve will tend to be of the form of a square law—i.e., a “modified” Child's law curve. Of course, except in the Ohm's law region, electrical conduction is space-charge-limited (SCL) in any case.

The present work presents: (a) the first complete experimental characterization of the bounding sides of Lampert's triangle in a single material, (b) a dramatic TFL verticality conforming to theory, and (c) a somewhat novel method, namely, neutron irradiation, of obtaining in *n*-type silicon the very high resistivity which is necessary for SCL studies.² This method was used simultaneously to introduce the necessary traps for obtaining the TFL characteristics.

THEORY

The Lampert triangle can be defined through a mathematically elegant process of limiting conditions and approximations³; however, the bounding sides may be simply arrived at by the use of the electron current flow equation

$$J = ne\mu E, \quad (1)$$

* Work supported by the National Science Foundation.

† Present address: University of Cincinnati, Department of Electrical Engineering, Cincinnati, Ohio 45221.

¹ M. A. Lampert, *Phys. Rev.* **103**, 1648 (1956).

² Highly purified silicon is inherently *p*-type owing to a residual boron content; therefore, all known single-carrier SCL experiments to date in silicon have been based upon *p*-type material.

³ See appendices of Ref. 1.

the single-dimensional form of Poisson's equation

$$dE/dx = \rho/\epsilon, \quad (2)$$

and the boundary conditions

$$\begin{aligned} E = -dV/dx = 0 & \quad \text{at } x=0 \text{ (cathode),} \\ V = 0 & \quad \text{at } x=0, \end{aligned} \quad (3)$$

where J is the current density, n is the volume density of free electrons, e is the magnitude of electron charge, μ is the electron mobility in silicon, x is the coordinate variable of the rectangular sample configuration, E is the applied electric field intensity along the x coordinate, ρ is the volume space charge density, ϵ is the dielectric permittivity of silicon, and V is the electrical potential.

Equation (1) neglects diffusive flow. The validity of this assumption is apparent in the Ohm's law region; however, the SCL region bears further consideration. The first boundary condition above necessitates diffusive flow at the cathode interface, but the diffusive contribution to the general current flow equation can be neglected if the sample thickness is many diffusion lengths thick. In that case, the current is drift dominated throughout most of the bulk, and Eq. (1) is appropriate. The literature shows that it is common practice to ignore diffusive flow in SCL injection

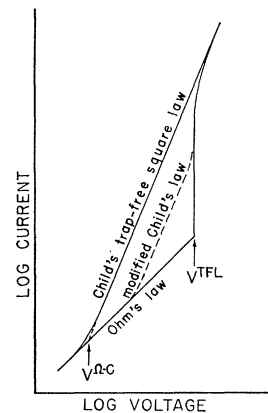


FIG. 1. Lampert's theoretical triangle, bounded by Ohm's law, Child's trap-free square law for solids, and the TFL region. A “modified” Child's law may be predicted for shallow traps.

studies, even to sample thicknesses of a few microns in silicon. Although such practice in those ranges of thickness is indeed questionable, use of only the drift term has been determined to be sufficiently accurate in the present work, since the minimum thickness is about 121 μ , and neutron irradiation has greatly reduced the carrier lifetime.

The first boundary condition is justified on the basis that appropriate Ohmic electrodes are employed so that conduction is bulk-limited by the material and not constrained by the electrodes. This means that there is an essentially infinite supply of electrons available at the cathode, and hence, from Eq. (1), the field is vanishingly small at $x=0$. The second boundary condition is arbitrary.

At low levels of injection, there will be no substantial deviation from the thermal-equilibrium electron density n_0 ; therefore $n \simeq n_0$, and Eq. (1) becomes

$$J = n_0 e \mu E = n_0 e \mu (V/L), \quad (4)$$

where L is the sample length. Equation (4) specifies the Ohm's law region and the lower bound of the Lampert triangle.

The upper bound of the triangle is determined as follows: In the absence of traps, all of the injected charge will enter the conduction band, and a space charge ρ will begin to build up as the injection level is increased. Then $\rho = -(n - n_0)e$ is approximated as $\rho \simeq -ne$ at high injection levels, where $n \gg n_0$. Thus, by replacing ρ by $-ne$ in Eq. (2) and substituting this expression into Eq. (1), the current density becomes

$$J = -\epsilon \mu E (dE/dx) \quad (5)$$

for the case of high-level SCL injection. After integrating Eq. (5) from the cathode at $x=0$ to some general point, consistent with the first boundary condition, and then solving the resulting field expression for the anode voltage at $x=L$, subject to the boundary conditions, the current density in the SCL mode in the absence of traps is extracted and expressed as

$$J = (9/8) \epsilon \mu V^2 / L^3. \quad (6)$$

Equation (6) is Child's trap-free square law for solids, first derived by Mott and Gurney,⁴ based upon the original work of Child.⁵

The onset of the SCL mode is, of course, somewhat gradual, but the extrapolated trap-free square law intersects the Ohm's law curve at

$$V^{\Omega-e} = (8/9) n_0 e L^2 / \epsilon \quad (7)$$

as determined by setting Eq. (1) equal to Eq. (6).⁶ Essentially, the same result is obtained by using the

criterion that the SCL mode begins when the injected (excess) charge becomes equal to the equilibrium density (i.e., $n \simeq 2n_0$). The latter criterion is reasonable, since at that point the charge perturbation becomes comparable to the charge concentration being perturbed, and beyond this point the injected excess charge predominates.

The third side of the triangle corresponds to the case where the thermal-equilibrium (unfilled) trap density $n_{t0} \gg n_0$. In this instance, essentially all of the electrons injected into the material will be trapped until the injected electron concentration becomes comparable to the trap density n_{t0} . At that point, the space-charge density may be expressed as $\rho \simeq -n_{t0}e$. Inasmuch as the trap density in this case greatly exceeds the thermal-equilibrium free-electron density (true for an insulator or semi-insulator), the space charge is essentially constituted of a trapped negative charge density, $-n_{t0}e$, at the TFL voltage V^{TFL} . Hence, the normal one-sided depletion-mode equation is applicable:

$$V^{\text{TFL}} = n_{t0} e L^2 / 2\epsilon. \quad (8)$$

Equation (8), which is identical to the results of Lampert's more involved analysis,³ may be very simply derived by double integration of the Laplacian form of Eq. (2), subject to the boundary conditions of (3).

Once the traps are filled, the remaining charge enters the conduction band, so a drastic increase in current occurs. In the same spirit of the earlier alternative perturbation criterion for $V^{\Omega-e}$, the TFL characteristic is expected to phase into the trap-free square law when $n \simeq n_{t0}$, which corresponds to $V \simeq 2V^{\text{TFL}}$.⁷ At that point, the free space charge begins to exceed and overshadow the trapped space charge, and the curve merges with the trap-free square-law curve.

Lampert's analysis indicates that the slope of the TFL line should be essentially vertical with

$$d(\ln I) / d(\ln V) \simeq n_{t0} / n_0. \quad (9)$$

The few observed cases of TFL behavior prior to the present paper have typically reported slopes rather less than the theoretical value; however, the present results are in almost exact agreement with Eq. (9).

STATE OF DEVELOPMENT

Certain relevant theoretical work on the trap-free case⁸ as well as the case of injection in the presence of traps⁹ was reported prior to Lampert's work of 1956. Also, some experimental work on CdS in the presence of traps had been earlier reported by Smith and Rose.¹⁰

⁴ N. F. Mott and R. W. Gurney, *Electronic Processes in Ionic Crystals* (Dover Publications, Inc., New York, 1964), 2nd ed., p. 172.

⁵ C. D. Child, *Phys. Rev.* **32**, 492 (1911).

⁶ Of course the Ohm's law expression $E = V/L$ is used in Eq. (1), and the concentration n becomes n_0 at the point of intersection.

⁷ This assumes a constant capacitance, which is shown by Lampert to be a reasonable approximation.

⁸ W. Shockley and R. C. Prim, *Phys. Rev.* **90**, 753 (1953).

⁹ A. Rose, *Phys. Rev.* **97**, 1538 (1955).

¹⁰ R. W. Smith and A. Rose, *Phys. Rev.* **97**, 1531 (1955).

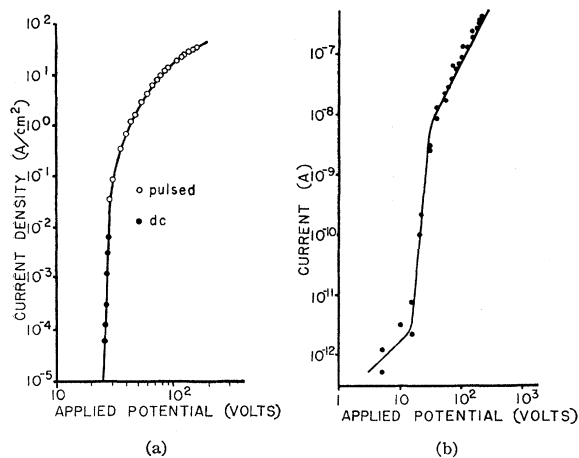


FIG. 2. (a) TFL behavior in a high-purity p^+-p-p^+ Si diode at 4.2°K, after Gregory and Jordan. (b) TFL behavior in ZnS (presumably at room temperature), after Ruppel.

Since 1956, many cases (e.g., Refs. 11–18) of SCL square-law behavior have been observed, either for the case of trap-free conduction of “modified” square-law behavior in the presence of traps (which is accommodated by the Lampert theory). Also, the case of SCL conduction with field-dependent mobility has been theorized^{19,20} and experimentally observed.^{17,21}

Owing to either a very low free-carrier density or the use of a $p-n$ junction for carrier injection, the Ohm’s law–Child’s law intercept has not often been observed. TFL-type behavior has been observed in perhaps less than a half-dozen cases—by Smith and Rose,¹⁰ by Lampert, Rose, and Smith,¹³ and by Bube¹⁵ in CdS; by Ruppel¹² in ZnS, and more recently by Gregory and Jordan²² in Si. Of these, Ruppel and Smith and Rose observed both an Ohm’s law region and a reasonably sharp transition to at least a portion of the TFL curve. In all cases, the TFL line was sufficiently non-vertical that points could be plotted throughout that region, despite the fact that Lampert’s theory predicts an essentially vertical line, as given by Eq. (9), for typical conditions.

The nonverticality of earlier results may in part have been a consequence of the difficulty in obtaining true values due to the length of time (sometimes hours) required to obtain steady-state readings in CdS and

ZnS. However, even in the results reported by Gregory and Jordan²² for Si, which represent the only previously reported TFL behavior in Si or any of the classical semiconductors, the slope as seen in Fig. 2(a) is certainly less than vertical.

Ruppel’s results in ZnS, as shown in Fig. 2(b), are very impressive in that they show three sides of a triangular region, if the square-law region is extrapolated back to the Ohm’s law line. However, the square-law region apparently cannot represent the third side of the Lampert triangle, because the line is reported by Ruppel to be many orders of magnitude below the theoretical trap-free line. (A possible explanation will be discussed later in view of the author’s observations.)

DEVICE

The diode used for this investigation was a silicon chip initially doped with phosphorus to 10^{14} cm^{-3} . The material was then irradiated to 1.1×10^{16} fast neutrons cm^{-2} (>0.1 MeV). The traps and other lattice damage, introduced as a consequence of irradiation, increased the resistivity to nearly 10^7 Ω cm at 77°K while maintaining the n -type character of the material.

The crystal had been pulled from a quartz crucible, so the oxygen content was expected to be of the order of 10^{17} – 10^{18} cm^{-3} .²³ It is well known that oxygen in silicon will become electrically activated after irradiation, resulting in electron traps (very deep acceptors) owing to the creation of an oxygen-vacancy-type complex. Other deeper electron traps are also created, as well as some very shallow electron traps near the conduction band, but the oxygen vacancy or “A center” is by far the most thoroughly documented trap in irradiated silicon. This trap has been variously reported to lie 0.15–0.18 eV below the conduction band edge E_c ; however, the most reliable data seem to point toward a value of about $E_c - 0.17$ eV.²⁴

It was found, using the normal Fermi function

$$n_0 = N_c e^{(E_F - E_c)/kT}, \quad (10)$$

where k is Boltzmann’s constant and T is the temperature absolute, that the above radiation dose biased the Fermi level E_F at $T=77^\circ\text{K}$, to $E_c - 0.17$ eV within experimental accuracy. This calculation was based upon appropriate resistivity measurements and extrapolated Hall measurements on a number of samples. Calculation of the effective density-of-states function N_c was based upon the work of McFarland *et al.*²⁵

The electrodes consisted of gold alloys deposited *in vacuo* upon carefully prepared (111) surfaces. A 0.85% Sb-Au cathode was separated by the wafer thickness of 121 μ , from a 3% Ga-Au anode. Experiments based upon electrode combinations showed the Ga-Au surface to be a relatively poor carrier injector. The latter fact,

¹¹ G. T. Wright, *Nature* **182**, 1296 (1958).

¹² W. Ruppel, *Helv. Phys. Acta* **31**, 311 (1958).

¹³ M. A. Lampert, A. Rose, and R. W. Smith, *J. Phys. Chem. Solids* **8**, 464 (1959).

¹⁴ R. D. Larabee, *Phys. Rev.* **121**, 37 (1960).

¹⁵ R. H. Bube, *J. Appl. Phys.* **33**, 1733 (1962).

¹⁶ H. Lemke, *Phys. Status Solidi* **16**, 427 (1966).

¹⁷ S. Denda and M. A. Nicolet, *J. Appl. Phys.* **37**, 2412 (1966).

¹⁸ U. Buget and G. T. Wright, *Solid-State Electron.* **10**, 199 (1967).

¹⁹ G. C. Dacey, *Phys. Rev.* **90**, 759 (1953).

²⁰ M. A. Lampert, *J. Appl. Phys.* **29**, 1082 (1958).

²¹ S. Okazaki and M. Hiramatsu, *Solid-State Electron.* **10**, 273 (1967).

²² B. L. Gregory and A. G. Jordan, *Phys. Rev.* **134**, A1378 (1964).

²³ W. Kaiser *et al.*, *Phys. Rev.* **101**, 1264 (1956).

²⁴ G. D. Watkins and J. W. Corbett, *Phys. Rev.* **121**, 1001 (1961).

²⁵ G. G. Macfarland *et al.*, *Phys. Rev.* **108**, 1377 (1957).

along with a hole barrier due to "giant" Coulombic hole traps,²⁶ the placement of the Fermi level, and the relatively low hole mobility, made single-carrier (electron) injection possible throughout the range of interest.²⁷ Appropriate surface band bending to achieve Ohmic contact at the cathode was obtained by application, where necessary, of a short pulse of high forward bias. Contact was made to the electrodes with room-temperature silver Epoxy to prevent annealing of the traps.

EXPERIMENTAL RESULTS

Figure 3 shows an experimental plot wherein one sees that the calculated trap-free square law fits into the experimental pattern very well. The trap-free curve is drawn by defining a point A by Eq. (7) and extending a line from that point with a slope of 2. The same curve may be defined by extending a line of slope 2 from point B at some arbitrary voltage (taken here as V^{TFL}), starting at the current density²⁸ calculated from Eq. (6). Within the experimental uncertainty, the value of mobility was chosen which would give a self-consistent trap-free line in the two above methods. However, a variation of an order of magnitude in mobility would not cause a serious disagreement in the two cases.

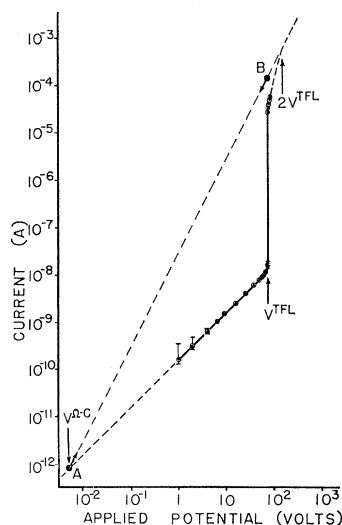


FIG. 3. Experimental evidence of Lampert's triangle in irradiated silicon at 77°K. The theoretical trap-free square law is defined at point A by Eq. (7), and the line is extended upward with a slope of 2. Similarly, the trap-free line is defined at some point B by Eq. (6) and extended upward with a slope of 2, giving a self-consistent line in the two cases. The range of values shown in the three lowest readings in the Ohm's law region is due to stabilization, and finally noise about a final mean.

²⁶ Created by the ionization of radiation-induced electron traps below the A center, as a result of the original donor concentration.

²⁷ It was found that double injection (holes and electrons) could be obtained at a lower neutron dose and consequently lower trapping concentration, even with symmetrical Sb-Au electrodes. These results are planned for a separate paper.

²⁸ The effective electrode area was calculated on the basis of a Kelvin resistivity measurement on the Hall bar and an arbitrary point in the Ohm's law region of the volt-ampere plot.

Perhaps the most striking feature of Fig. 3 is the extreme verticality of the TFL slope. A high-resolution digital voltmeter made it possible to record the difference in voltage between the bottom and top of the vertical portion of the TFL line, resulting in a calculated slope of about 1.5×10^4 . This may be compared with a theoretical value of 2.1×10^4 based upon Eq. (9), where the A-center trap density n_{t0} was determined from Eq. (8) after substituting the observed value for V^{TFL} , and n_0 was determined to be $2.8 \times 10^8 \text{ cm}^{-3}$ based upon resistivity and Hall measurements.

The theory as discussed by Lampert¹ concludes that the TFL behavior should occur when the controlling trap lies sufficiently below the normal thermodynamic Fermi level that it may be classified as a deep trap. However, at 77°K we have that kT is less than 0.007 eV, so the experimental uncertainty in the relative location of the Fermi level and the A center could easily accommodate a few kT , thus giving the A center the appearance of a relatively deep trap at this temperature.

The Lampert theory indicates that if the controlling trap is shallow (sufficiently above the thermodynamic Fermi level), a square-law region will supersede the TFL line. (Such behavior would correspond to the "modified" Child's law curve of Fig. 1.) As the free-electron concentration increases, the steady-state Fermi level²⁹ (SSFL) rises. Thus, if any additional traps exist above the trap which is responsible for the observed behavior, the upper end of the TFL line would be expected to become a square law as the next trap is approached, then another TFL line would be expected as the SSFL moves up through that trap, filling it, then causing that trap in turn to appear deep as the SSFL moves on toward the conduction band. Similarly, one would expect a TFL line for each discrete trap through which the SSFL moves.

Inspection of Fig. 3 reveals that there appears to be no room in the Lampert triangle to accommodate additional TFL behavior, so there should be no additional traps above the one responsible for the observed TFL line. This is consistent with the literature, which generally reports the silicon A center as the most shallow electron trap in irradiated silicon, aside from one or more traps at about $E_c - 0.03 \text{ eV}$ (which would not be effective at this temperature). This reasoning lends additional confirmation to the validity of the original assertions.

In view of this argument, it is possible that the early onset of square-law behavior in ZnS following the TFL line in Fig. 2(b), as reported by Ruppel, was due to the existence of other traps lying nearer the conduction band.

The authors have, in fact, observed, in the same basic silicon material, what appears to be a multiple

²⁹ Defined as the normal thermodynamic Fermi level in Eq. (10), except n_0 is replaced by the total free-electron concentration n . See Ref. 1.

TFL behavior. However, this behavior was observed at a higher temperature, where lower-level traps would be effective, and these traps have not yet been identified.

A calculation of the A-center trap density, based on Eq. (8), gives a value of approximately $6 \times 10^{12} \text{ cm}^{-3}$. However, n_{i0} is actually the unfilled trap density below the Fermi level under the condition of thermal and electrostatic equilibrium. Therefore, it is possible that n_{i0} could be somewhat greater than the A-center density if additional unfilled levels exist below the A center, and it is possible that n_{i0} could be somewhat less than the A center density if a portion of the A-center traps were filled in thermal equilibrium. However, from tests on another similarly irradiated sample at a temperature where a definite modified square law could be observed (indicating that the Fermi level was below the trap and, therefore, that the trap was essentially empty in equilibrium in that case), a value was calculated to agree within 28% of the above value. This disagreement can be accounted for in the uncertainty in effective device length, which was determined by previously established etch rates. The TFL voltage is a very sensitive function of the length, being theoretically dependent upon the square of this dimension. Therefore, it is believed that the above figure for the trap density is of the proper order of magnitude. The introduction rate of the A center is thus approximately 6×10^{-4} traps/ n cm.

As expected, the onset of the TFL region can be arbitrarily suppressed by increasing the intensity of incident light of the proper wavelength. Quantitative aspects of this sensitivity are presently under investigation.

SIMILARITY WITH PUNCH-THROUGH

The volt-ampere characteristics at and above V^{TFL} are similar to those reported for Ge³⁰ and Si¹⁷ just beyond punch-through in p - π - p and n - π - n structures, respectively, owing to the reverse biased junction. Here, π represents a high-resistivity n -type region in the first case, while π represents a high-resistivity p -type region in the latter. The rapid increase in current in these experiments is due to the additional charge required to establish the increasing voltage after the depletion region has extended to a maximum.

In fact, the rapid increase in current in the above cases occurs at a voltage across the reverse biased junction which is identical to that described by Eq. (8), if n_{i0} is replaced by the impurity density. Thus, the punch-through voltage and the TFL voltage are somewhat analogous, although arising from different causes. However, the region above these characteristic voltages corresponds to a trap-free SCL injection in both cases.

³⁰ A. Shumka and M. A. Nicolet, in *Proceedings of the Seventh International Conference on the Physics of Semiconductors, Paris, 1964* (Academic Press Inc., New York, 1965), p. 621.

As noted in Refs. 17 and 30, onset of (trap-free) SCL conduction may not lead to square law, because of field dependence in the mobility and the eventual onset of velocity saturation. Certainly, the region above V^{TFL} in Fig. 3 is near the $\mu \propto E^{-1/2}$ range for silicon, and one cannot be certain that the curve is actually approaching a square-law dependence, based on the limited number of data points presented. However, there is no sublinear Ohm's law region, so the above possibility does not affect the application of the Lampert theory in explaining the bounding sides of the triangle, although nonconstant mobility may perturb the shape of the upper tip of the enclosed region.

CONCLUSIONS AND PROJECTIONS

The Lampert theory for single-carrier injection, in terms of the bounding sides of the Lampert triangle, is supported by the observed SCL conduction characteristics in fast-neutron-irradiated silicon. The limited number of data above the TFL region does not completely and unambiguously establish that the upper region is a square law, but this fact does not alter the validity of the Lampert theory in the triangular region in any case. Certainly a line of unity slope intersects the TFL line, so no significant field dependence of mobility appears at that point.

It is hoped that future pulsed measurements in this upper region will allow additional data points without significant heating; however, a continuum of shallow traps near the conduction band would be expected to distort the simple square-law behavior as the SSFL intersects this upper region of the band gap near the conduction band, in addition to possible modification because of field-dependent mobility.

Perhaps most dramatic in this experiment is the TFL region, which possesses the anticipated verticality.

Extension of this high-level injection method to the case of multiple TFL behavior for separate electron- and hole-injection experiments potentially provides a simple and powerful tool for probing the band gap, as the SSFL sweeps upward (electron injection) or downward (hole injection) through the gap with increasing applied voltage. A TFL voltage may be anticipated for each discrete trap through which the SSFL passes.

The extensive physical controllability of V^{TFL} as indicated by Eq. (8) and the observed optical sensitivity of V^{TFL} also suggest a number of potentially useful device applications.

ACKNOWLEDGMENTS

We wish to express our appreciation to the staff of the Air Force Nuclear Engineering Test Facility of the Air Force Institute of Technology at Wright-Patterson Air Force Base, Ohio, for providing the nuclear irradiation facilities. Particular thanks are extended to the project engineer, A. R. Bauer, and to W. D. Rogers, who provided the final dosimetry analysis.